Efficient removal of Malachite Green from aqueous solution by adsorption on carbon nanotubes modified with ZnFe$_2$O$_4$ nanoparticles

SHIVA DEHGHAN ABKENAR[1]*, MORASSA HASSANNEZHAD[2], MORTEZA
HOSSEINI[3] and MOHAMMAD REZA GANJALI[2,4]**

*[1]Department of Chemistry, Savadkooh Branch, Islamic Azad University, Savadkooh, Iran,
[2]Center of Excellence in Electrochemistry, Faculty of Chemistry, University of Tehran,
Tehran, Iran, [3]Department of Life Science Engineering, Faculty of New Sciences &
Technologies, University of Tehran, Tehran, Iran and [4]BiosensorResearch Center,
Endocrinology and Metabolism Molecular-Cellular Sciences Institute, Tehran
University of Medical Sciences, Tehran, Iran*

Abstract. In this study, multiwall carbon nanotubes modified with spinel zinc ferrite nanoparticle (ZnFe$_2$O$_4$/MWCNTs) were used as a solid phase adsorbent for the removal of Malachite Green (MG) from aqueous media. The synthesized nanocomposite was characterized by different methods, such as Fourier transform infrared spectroscopy (FT-IR), scanning electron microscopy (SEM) and X-ray diffraction (XRD). Batch adsorption experiments to determine the optimal adsorption conditions and different factors that influence the adsorption efficiency (*i.e.*, pH, amount of adsorbent, contact time, and the initial concentration of MG) were also evaluated and optimized. The data were satisfactorily fitted to the Langmuir model and a maximum adsorption capacity of 116.2 mg g^{-1} was obtained at a pH of 7.5. In addition, adsorption kinetics studies were performed. The adsorption of the model dye (MG) was found to reach equilibrium after 60 min, following a pseudo-second-order kinetic model. Furthermore, an external magnetic field could easily separate the nanoparticles from water with a high separation efficiency.

Keywords: dye removal; Malachite Green; modified multiwall carbon nanotubes; spinel zinc ferrite nanoparticle.

INTRODUCTION

Water is one of the necessities required for the sustenance and continuation of life. It is therefore imperative that a water supply of good quality be available for various activities. However, this is becoming increasingly difficult considering the large-scale pollution caused by industrial, agricultural and domestic acti-

vities. These activities generate wastewater that contains both inorganic and organic pollutants. Some of the common pollutants are phenols, dyes, detergents, insecticides, pesticides and heavy metals.[1]

Removal of dyes from waste waters has recently received considerable attention and a range of methods, such as adsorption, flocculation, oxidation and electrolysis, has been developed.[2–4] Among these approaches, adsorption techniques offer simple, yet effective and economical tools for treating wastewaters.[5,6] The unique physicochemical qualities of nanomaterials, including their considerable surface area and the large number of defective sites present in their structure, are expected to result in enhanced uptake and adsorption properties, in comparison to their micro-sized counterparts.[7–10]

Malachite Green (MG) is a triarylmethane dye that has been controversially applied in the aquaculture industry to treat and prevent protozoa and fungal infections.[11] MG is potentially carcinogenic, mutagenic, teratogenic, and toxic and thus it is classified as a class II health hazardous material by the Occupational Safety and Health Administration (OSHA, USA).[12] The acute oral LD_{50} (lethal dose, 50 %) values of MG in rats have been reported to be 275–520 mg kg^{-1} body weight. Although MG has been banned in most countries, it is still used in many parts of the world because of its high efficacy, low cost, and availability, as well as the existence of less restrictive laws for non-aquaculture purposes.[11]

In recent years, multiwall carbon nanotubes (MWCNTs) have attracted considerable attention due to their unique structure and properties, including large surface areas, high aspect ratios, nanosized stability and rich surface chemical functionalities. However, MWCNTs are very hydrophobic and easily aggregate in aqueous solution because of strong van der Waals interaction forces between MWCNTs, which may hinder effective adsorption behaviors and reduce the adsorption capacity.[13,14] Therefore, decoration of MWCNTs by the introduction of inorganic nanoparticles is an effective way to enhance their dispersibility and performance.[15]

Spinel ferrites nanoparticles, with the general formula MFe_2O_4 (M = Fe, Co, Cu, Mn, Zn, *etc.*), are of the most popular magnetic materials in analytical chemistry and can improve electrochemical, optical and magnetic properties of carbon based nanomaterials, such as carbon nanotubes (CNTs),[16] graphene oxide[17] and graphene quantum dots.[18]

Zinc ferrite nanoparticle ($ZnFe_2O_4$ NP), as one of the spinel ferrite compounds; have attracted increasing interest because of their good biocompatibility, low toxicity, electrical properties, easy synthesis and high adsorption ability.[19] In order to effectively utilize the advantages of both ferrite nanoparticles and carbon nanotubes, various kinds of modified CNTs have been synthesized by decorating CNTs with nanoparticles, such as $CoFe_2O_4$,[20] $NiFe_2O_4$[21] and $MnFe_2O_4$.[22]

In the present study, multiwall carbon nanotubes modified with spinel zinc ferrite nanoparticle ($ZnFe_2O_4$/MWCNTs) were synthesized and then assessed as the adsorbent for MG removal from water. The $ZnFe_2O_4$/MWCNTs could be easily separated by an external magnetic field. Influencing factors, including pH, time and the initial concentration, on the MG adsorption efficiency were investigated. The adsorption kinetics were studied. In addition, the adsorption efficiency and mechanism were assessed based on isothermal studies.

EXPERIMENTAL

Instruments

Spectrophotometric measurements were realized with a Perkin Elmer (Lambda 25) double-beam spectrophotometer for monitoring the MG concentration. All the pH values were measured with a Lab 850 Benchtop pH meter. The IR spectra were taken using a Fourier transform infrared spectrometer (FT-IR; Perkin Elmer, USA).

Scanning electron microscopy (SEM) images were taken with a KYKY-EM3200 digital scanning electron microscope operated at 26 kV.

The morphological analysis by X-ray diffraction was performed on an XPert MPD advanced diffractometer using $Cu(K_\alpha)$ radiation at room temperature in the 2θ range from 4 to 120° at a scanning rate of 0.02° s^{-1}.

Chemicals and reagents

Reagent-grade compounds were procured from Fluka and Merck and double distilled water (DDW) was used in all steps of the study. The glassware used for trace analysis were maintained in diluted nitric acid for at least one day and then washed repeatedly with DDW, prior to application. Multi-walled carbon nanotubes (purity >95 %) were purchased from Shenzhen Nanotech Port Co. and zinc nitrate ($Zn(NO_3)_2 \cdot 6H_2O$) and ferric nitrate ($Fe(NO_3)_3 \cdot 9H_2O$) were obtained from Sigma–Aldrich (St. Louis, MO, USA). The MG stock solution was obtained through dissolving the dye powder in DDW. The other solutions were obtained through diluting stock solution to the desired concentrations.

Synthesis of $ZnFe_2O_4$/MWCNTs nanocomposite

The $ZnFe_2O_4$ nanoparticles on carboxyl functionalized MWCNTs were fabricated by a hydrothermal process. In order to synthesize carboxyl functionalized MWCNTs, the pure MWCNTs were refluxed in a mixture of concentrated sulfuric acid and nitric acid (3:1 volume ratio) at 70 °C for 6 h. After cooling to room temperature, the product was washed with double distilled water several times until the pH of the filtrate was ≈7 and finally dried at 60 °C for 24 h. The prepared carboxyl functionalized MWCNTs were used as templates for the formation of the $ZnFe_2O_4$/MWCNTs nanocomposite. Then, certain quantities of the carboxyl functionalized MWCNTs was weighed and dispersed in mixture of 15 mL ethanol and 5 mL acetonitrile, through sonication in an ultrasound bath for 50 min. Thereafter, 0.35 g of $Fe(NO_3)_3 \cdot 9H_2O$ and 0.12 g $Zn(NO_3)_2 \cdot 6H_2O$ were added to the solution while stirring for 60 min at room temperature. During this process, positively charged Fe^{3+} and Zn^{2+} can be absorbed on the hydroxyl and carboxyl groups on the surface of the negatively charged carboxyl functionalized MWCNTs by electrostatic attraction. Then 1 mL of NaOH (0.1 M) solution was added into the above solution under stirring. Upon the addition of NaOH solution, the hydrolysis of Fe^{3+} and Zn^{2+} leads to the formation of $ZnFe_2O_4$ nanoparticles deposited on the surface of the MWCNTs. After 1 h of stirring, the formed dark brown suspension was cen-

trifuged and the solid product was separated, washed with a water and ethanol mixture. The formed dark brown precipitate was dispersed in 25 mL water while sonicating, transferred to a 50 mL autoclave, and treated at 180 °C for 12 h. The resulting powder was denoted as $ZnFe_2O_4$/MWCNTs nanocomposite.

MG adsorption experiments

The $ZnFe_2O_4$/MWCNTs were used to adsorb Malachite Green from water samples and all experiments were performed in triplicate. Equilibrium experiments involved adding 0.010 g of $ZnFe_2O_4$/MWCNTs to 10 mL of a 50 mg L^{-1} of MG solution (pH 7.5). The mixtures were gently shaken for 60 min under ambient conditions and subsequently, the magnetic nanoparticles with adsorbed dyes were separated from the mixture *via* a permanent hand-held magnet. Before, during and after the adsorption experiments, the MG concentration was determined through spectrophotometry at 616.5 nm. From the obtained data, the dye removal efficiency was calculated using the following equations:

$$R\,/\,\% = 100\frac{c_0 - c_t}{c_0} \tag{1}$$

where c_0 and c_t are the initial MG concentration and the concentration at the end of the experiment at time t.

The experiments also involved evaluating the effects of pH, the amount of $ZnFe_2O_4$/ /MWCNTs, contact time, and initial MG concentration on the adsorption efficiency. Furthermore, the kinetics of the adsorption phenomenon was evaluated through monitoring the adsorption capacity at various intervals. To obtain the adsorption isotherms, the dye solutions within the initial concentrations in the range of 10–200 mg L^{-1} were used in adsorption experiments until equilibrium conditions.

The amounts of the adsorbed MG (q_e) of dye were calculated using the following equation:

$$q_e = \frac{c_0 - c_e}{m}V \tag{2}$$

where c_0 and c_e represent the initial and equilibrium MG concentrations, m is the mass of $ZnFe_2O_4$/MWCNTs, and V is the solution volume.

<div align="center">RESULTS AND DISCUSSION</div>

Characterization of nanocomposite

FT–IR was used to ascertain the presence of carboxyl functionality on MWCNTs, and to check the presence of $ZnFe_2O_4$ nanoparticles on the surface of MWCNTs (Fig. 1). In the spectrum of carboxyl functionalized MWCNTs (curve a) the peaks at 1640 and 1382 cm^{-1} correspond to C=O and C–O stretching, respectively. The two weak peaks at 2935 and 2840 cm^{-1} correspond to the –CH stretching mode and a broad band peak at 3440 cm^{-1} is attributed to the carboxylate groups on the external surface of MWCNTs.[23] Compared with the spectrum of $ZnFe_2O_4$/MWCNTs (curve b), the peaks at around 620 and 1153 cm^{-1}, which are assigned to the deformation of different types of C–H bonds and formation of COOH groups,[24,25] were shifted to higher wavenumbers. This observation indicates the bonding of $ZnFe_2O_4$ to C–O–H groups on the surface of

MWCNTs. In curve b, the new bands at 1385 and 820 cm^{-1} are due to the stretching of Zn–O–Fe bonds of the tetrahedral building units forming the spinel ferrite structure. In addition, the peak at 590 cm^{-1} could be attributed to the stretching vibration of the Fe–O bond.[23]
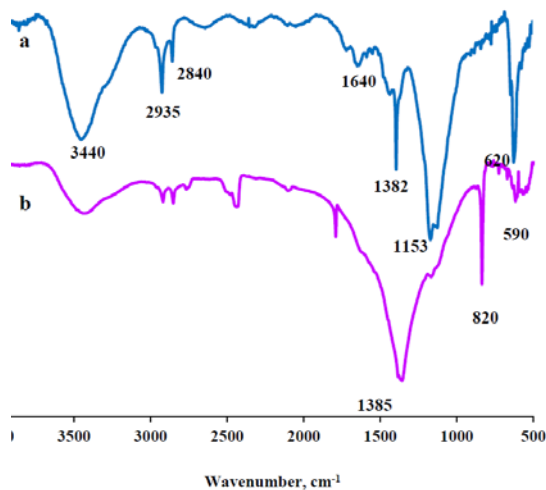
Fig. 1. FT-IR spectra of carboxyl functionalized MWCNTs (a) and ZnFe$_2$O$_4$/ /MWCNTs (b).

The phase and crystalline structure of the pure MWCNTs as well as the synthesized ZnFe$_2$O$_4$/MWCNTs nanocomposite was investigated by their powder X-ray diffraction pattern, shown in Fig. 2. The XRD pattern of pure MWCNTs shows one obvious peak at 2θ of 24°, which corresponds to the (002) plane of
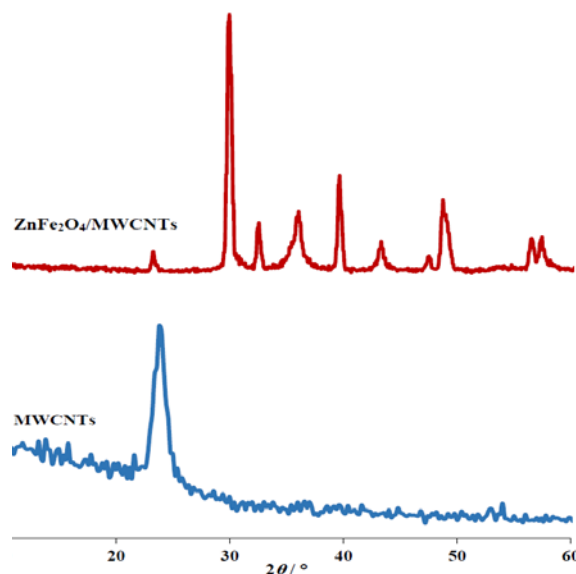
Fig. 2. XRD pattern of pure MWCNTs and ZnFe$_2$O$_4$/MWCNTs.

MWCNTs. For the XRD pattern of the $ZnFe_2O_4$/MWCNTs nanocomposite, the presence of six diffraction peaks at 2θ values of 30, 35.65, 39.25, 43, 56 and 57°, corresponding to the reflection planes (220), (311), (222), (400), (422) and (511), respectively, confirm the formation of the spinel structure of $ZnFe_2O_4$.[26] The XRD result indicates that the synthesized nanocomposite contained MWCNTs and $ZnFe_2O_4$ nanoparticles.

In order to obtain information about the surface morphologies of the MWCNTs before and after the modification process, SEM images were taken. As shown in Fig. 3A, pure MWCNTs have almost homogeneous structures with a smooth surface. However, the $ZnFe_2O_4$ nanoparticles are well distributed on the surface of MWCNTs, producing no change in the morphology of the Multi-walled carbon nanotubes, only modifying it (Fig. 3B).
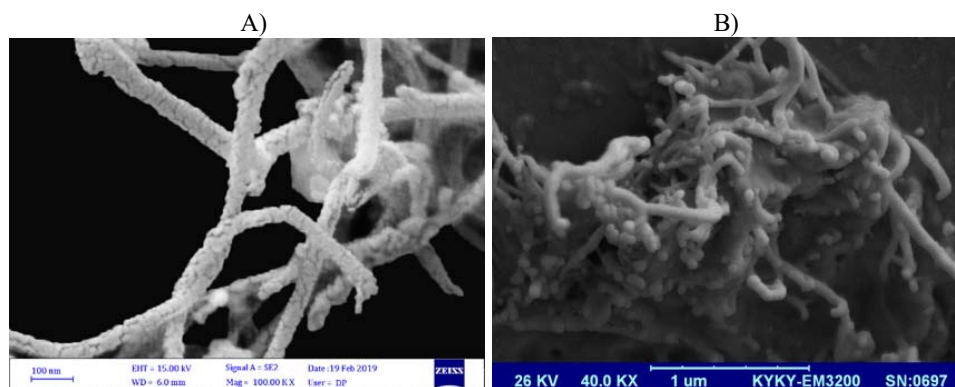
Fig. 3. SEM images of: A) pure MWCNTs and B) $ZnFe_2O_4$/MWCNTs.

Effect of pH

The pH of the dye solution plays a crucial role in the whole adsorption process because the pH may affect both the aqueous chemistry and surface binding sites of the adsorbent. In order to determine the best pH, studies were performed in the pH range of 3.0 to 10.0 with fixed initial concentration and contact time onto an exactly weighed amount of adsorbent (10 mg). The results are given in Fig. S-1 of the Supplementary material to this paper. MG is known to exist in the cationic form in aqueous media and is hence attracted to negatively charged surfaces. According to the results, the adsorption of MG was increased at higher pH values until 8.0 and then decreased on increasing the pH. Hence, pH 7.5 was chosen for subsequent experiments. This phenomenon could be explained based on added negative charges on the surface of the nanoparticles, which could enhance the electrostatic interaction of nanoparticles and the cationic dye MG. At acidic pH, the decrease in adsorption could be explained by the fact that H^+ may compete with dye ions for the adsorption sites of adsorbent, thus inhibiting the

adsorption of dye[27] and in alkaline pH, OH⁻ could be absorbed by MG, and the resulting electrostatic repulsion could negatively influence the adsorption.

Effect of the amount of adsorbent on the removal efficiency

The effect of the amount of $ZnFe_2O_4$/MWCNTs on the removal of MG reaching the optimal adsorption efficiency was determined by varying the adsorbent amount in the range of 0.002 to 0.015 g, in 10 mL sample containing 50 mg L⁻¹ MG at pH 7.5. Based on the results, the removal efficiency increased on increasing the amount of $ZnFe_2O_4$/MWCNTs, which corresponds to the presence of more adsorption sites and their availability. The solution containing 0.006 g adsorbent had a removal efficiency of 90 % and the adsorption reached maximum with 0.010 g of adsorbent with maximum percentage removal of about 93 %.

Effect of contact time

The influence of contact time on the adsorption efficiency was studied at an initial MG concentration of 50 mg L⁻¹ and the amount of the adsorbent of 0.010 g. The concentration of dye in the solution at different times (after 5, 10, 20, 40 and 60 min) was spectrophotometrically determined. The results (Fig. S-2 of the Supplementary material) clearly indicate that the adsorption capacity initially rapidly increases, and then continues to increase at a relatively slow speed and after about 60 min, the total dye content of the sample was adsorbed. To determine the adsorption mechanism, a pseudo first-order and a pseudo-second-order kinetic model were used to fit the experimental data.

The pseudo-first-order model is described by the Lagergren Equation:[28]

$$\log(q_e - q_t) = \log q_e - \frac{k_1 t}{2.303} \tag{3}$$

where k_1 is the pseudo-first-order rate constant, and q_e and q_t are the amount of absorbed MG at equilibrium and at time t, respectively.

The pseudo-second-order model, on the other hand, is expressed as:[29]

$$\frac{t}{q_t} = \frac{1}{k_2 q_e^2} + \frac{t}{q_e} \tag{4}$$

where k_2 / g mg⁻¹ min⁻¹ is the rate constant of the pseudo-second-order adsorption, and q_e and q_t are as given above.

The kinetic constants were obtained through linear regression for the two models (Fig. S-3 of the Supplementary material) and the results are presented in Table I. The correlation coefficient (R^2) of the pseudo-first-order kinetic model was rather low and the q_e values ($q_{e,cal}$) calculated from this model did not show good agreement with the experimental data ($q_{e,exp}$), reflecting the fact that the model is not appropriate. In the case of the pseudo-second-order model, on the other hand, R^2 was 0.9976 and the $q_{e,cal}$ values were in good agreement with the

$q_{e,exp}$ values, indicating the applicability of the kinetic model to the adsorption of MG onto ZnFe$_2$O$_4$/MWCNTs. The present findings are in good agreement with earlier reports.[30–35]

TABLE I. Adsorption kinetic parameters of MG adsorption on ZnFe$_2$O$_4$/MWCNTs

Pseudo-first order			Pseudo-second order			Experimental data
K_1 / min^{-1}	$q_{e,cal}$ / mg g^{-1}	R^2	K_2 / g mg^{-1} min^{-1}	$q_{e,cal}$ / mg g^{-1}	R^2	$q_{e,exp}$ / mg g^{-1}
0.0110	4.63	0.9598	0.01635	48.78	0.9976	48.52

Effect of the initial MG concentration

The effect of the initial concentration of MG in the solution on the adsorption capacity was studied at different MG concentrations in the range of 10–200 mg L^{-1}. The experiment was performed with a fixed adsorbent dosage, together with a firmly maintained temperature, under the optimum pH condition. The adsorption capacity for MG dye increased with increasing initial MG dye concentration in solution. A plot of adsorption capacity *vs*. MG concentration is illustrated in Fig. 4. Obviously, increasing concentration enhances the interaction between the dye and adsorbent, which could be attributed to the driving force created by the strong concentration gradients. Adsorption increases while the surface of the adsorbent is not saturated. Naturally, after all the adsorption sites are occupied, further increasing in the MG concentration does not increase the adsorption efficiency. In this study, Langmuir and Freundlich models were applied to fit the adsorption properties of the nanoparticles. The former model is based on assuming that the homogeneous sites of the adsorbent are covered by a monolayer of the dye molecule and that no species can be adsorbed after saturation is reached.[36] The Freundlich isotherm model, on the other hand, uses an empirical equation to describe heterogeneous systems.[37]
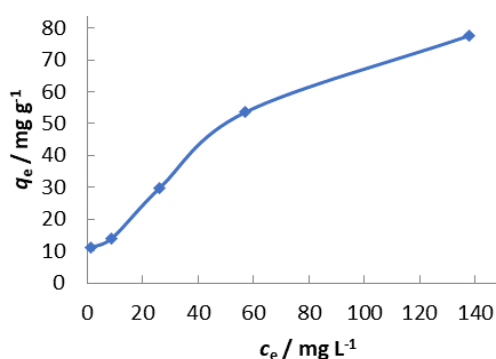
Fig 4. The effect of MG concentration on the dye adsorption capacity of ZnFe$_2$O$_4$/MWCNTs.

The linearized expression of the Langmuir model is given by:

$$\frac{c_e}{q_e} = \frac{1}{bq_m} + \frac{c_e}{q_m} \tag{5}$$

in which q_m is the highest adsorption capacity (reached when a monolayer completely covers the surface) and b expresses the equilibrium constant (L mg^{-1}).

The linearized form of the Freundlich is expressed as:

$$\log q_e = \log k_f + \frac{1}{n_f} \log c_e \tag{6}$$

k_f and $1/n_f$ being a rough indicator of the adsorption capacity, and the adsorption intensity, respectively. The slope $1/n_f$ ranges between 0–1 and reflects the adsorption intensity or surface heterogeneity. Closer to zero, $1/n_f$ values reflect higher heterogeneity of the surface.[38] These constants, determined using linear regression analysis, are given in Table II, illustrating the Langmuir isotherm as fitting since it exhibits a higher R^2 value compared to the Freundlich model. The maximum adsorption capacity was found to be 116.2 mg g^{-1}. It could be seen form Table III that the adsorption capacity of ZnFe$_2$O$_4$/MWCNTs is higher than that of many other previously reported adsorbents.

TABLE II. Isotherm parameters for the adsorption of MG on ZnFe$_2$O$_4$/MWCNTs

Dye	Langmuir			Freundlich		
	q_m / mg g^{-1}	b / L mg^{-1}	R^2	K_f / mg g^{-1}	$1/n$	R^2
MG	116.2	0. 0143	0.9933	3.57	0.6433	0.9851

TABLE III. Comparison of the maximum capacity factor of MG on various adsorbents

Adsorbent	Capacity factor, mg g^{-1}	Ref.
ZnFe$_2$O$_4$/MWCNTs	116.2	This work
CoFe$_2$O$_4$–SiO$_2$	75.5	2
Chitosan ionic liquid beads	8.07	1
Cellulose modified with phthalic anhydride	111.0	30
Activated carbon/CoFe$_2$O$_4$ composite	89.29	31
ZnO Nanorod-loaded activated carbon	66.68	32
Graphene oxide /cellulose bead	30.09	33
Copper sulfide nanorods loaded on activated carbon	145.98	34
Almond gum	196.07	35

CONCLUSIONS

In this study, the multi-walled carbon nanotubes modified with spinel ferrite ZnFe$_2$O$_4$ nanoparticles was prepared and employed as an adsorbent with great efficiency for MG removal from water. The equilibrium data were analyzed using the Langmuir and Freundlich isotherm models. The results showed the adsorption of MG on ZnFe$_2$O$_4$/MWCNTs follows the Langmuir adsorption

model with a maximum adsorption capacity of 116.2 mg g^{-1}. Adsorption kinetics of the process was found to follow a pseudo-second-order kinetic model. In addition, the cost of nanoparticle preparation is low, the functionalization is available easily, and the process of purifying water pollution is clean and safe using magnetic nanomaterials. All of these results indicate that this methodology could be used as a highly effective method for the removal of Malachite Green from aqueous solutions.

SUPPLEMENTARY MATERIAL

Additional data are available electronically from Journal web site http:// //www.shd.org.rs/JSCS/, or from the corresponding author on request.

И З В О Д

ЕФИКАСНО УКЛАЊАЊЕ МАЛАХИТО ЗЕЛЕНОГ ИЗ ВОДЕНИХ РАСТВОРА АДСОРПЦИЈОМ НА УГЉЕНИЧНИМ НАНОТУБАМА МОДИФИКОВАНИМ ZnFe$_2$O$_4$ НАНОЧЕСТИЦАМА

SHIVA DEHGHAN ABKENAR[1], MORASSA HASSANNEZHAD[2], MORTEZA HOSSEINI[3]
и MOHAMMAD REZA GANJALI[2,4]

[1]*Department of Chemistry, Savadkooh Branch, Islamic Azad University, Savadkooh, Iran,* [2]*Center of Excellence in Electrochemistry, Faculty of Chemistry, University of Tehran, Tehran, Iran,* [3]*Department of Life Science Engineering, Faculty of New Sciences & Technologies, University of Tehran, Tehran, Iran u* [4]*BiosensorResearch Center, Endocrinology and Metabolism Molecular-Cellular Sciences Institute, Tehran University of Medical Sciences, Tehran, Iran*

У овом раду су вишеслојне угљеничне нанотубе модификоване спинелним цинк-феритним наночестицама (ZnFe$_2$O$_4$/MWCNTs) коришћене као чврсти адсорбент за уклањање малахито зеленог (MG) из водене средине. Синтетисани нанокомпозит је окарактерисан различитим методама, као што су инфрацрвена спектроскопија са Фуријеовом трансформацијом (FT-IR), сканирајућа електронска микроскопија (SEM) и дифракција X-зрачења. Оптимални услови адсорпције одређени су експериментима равнотежне адсорпције. Испитиван је и оптимизован утицај различитих фактора на адсорпциону ефикасност (тј. pH, количина адсорбента, време контакта, и полазна концентрација MG), подаци су успешно фитовани Ленгмировим моделом и одређен је максимални адсорпциони капацитет од 116,2 mg g^{-1} на pH 7,5. Такође, извршено је испитивање адсорпционе кинетике. Одређено је да се адсорпциона равнотежа у случају модел молекула боје (MG) успоставља након 60 min, пратећи кинетички модел псеудо-другог реда. Додатно, спољашње магнетно поље успешно одваја наночестице од воде са високом ефикасношћу сепарације.

(Примљено 28. децембар 2018, ревидирано 17. априла, прихваћено 25. априла 2019)

REFERENCES

1. F. Naseeruteen, N. S. Abdul Hamid, F. Bukhari, M. Suah, W. S. Wan Ngah, F. Shimal Mehamod, *Int. J. Biol. Macromol.* **107** (2018) 1270 (https://doi.org/10.1016/j.ijbiomac.2017.09.111)

2. M. Amiri, M. Salavati-Niasari, A. Akbari, T. Gholami, *Int. J. Hydrogen Energy* **42** (2017) 24846 (https://doi.org/10.1016/j.ijhydene.2017.08.077)
3. M. Wawrzkiewicz, *Solvent Extr. Ion Exc.* **30** (2012) 507 (https://doi.org/10.1080/07366299.2011.639253)
4. G. Crini, *Bioresour. Technol.* **90** (2003) 193 (https://doi.org/10.1016/S0960-8524(03)00111-1)
5. C. D. Shuang, P. H. Li, A. M. Li, Q. Zhou, M. C. Zhang, Y. Zhou, *Water Res*. **46** (2012) 4417 (https://doi.org/10.1016/j.watres.2012.05.052)
6. S. D. Abkenar, M. Khoobi, R. Tarasi, M. Hosseini, A. Shafiee, M. R. Ganjali, *J. Environ. Eng*. **141** (2015) 04014049 (https://ascelibrary.org/doi/10.1061/(ASCE)EE.1943-7870.0000878)
7. B. Maddah, S. S. Javadi, A. Mirzaei, M. Rahimi-Nasrabadi, *J. Liq. Chromatogr. Relat. Technol.* **38** (2015) 208 (https://doi.org/10.1080/10826076.2014.896820)
8. F. Salehnia, M. Hosseini, M.R. Ganjali, *Microchim. Acta* **184** (2017) 2157 (https://doi.org/ 10.1007/s00604-017-2130-6)
9. H. R. Naderi, M. R. Ganjali, P. Norouzi, *Int. J. Electrochem. Sci.* **11** (2016) 4267 (https://doi.org/10.20964/2016.06.60)
10. M. Rahimi-Nasrabadi, S. M. Pourmortazavi, M. R. Ganjali, P. Norouzi, F. Faridbod, M. SadeghpourKarimi, *J. Mater. Sci. Mater. Electron.* **28** (2017) 3325 (https://doi.org/10.1007/s10854-016-5926-y)
11. S. C. Wei, S. Fan, C. W. Lien, B. Unnikrishnan, Y. S. Wang, H. W. Chu, C. C. Huang, P. H. Hsu, H. T. Chang, *Anal. Chim. Acta* **1003** (2018) 42 (https://doi.org/10.1016/j.aca.2017.11.076)
12. S. Srivastava, R. Sinha, D. Roy, *Aquat. Toxicol.* **66** (2004) 319 (https://doi.org/10.1016/j.aquatox.2003.09.008)
13. M. Sundararajan, S. K. Ghosh, *J. Phys. Chem., A* **115** (2011) 6732 (https://doi.org/10.1021/jp203723t)
14. F. Belloni, C. Kütahyali, V. V. Rondinella, P. Carbol, T. Wiss, A. Mangione, *Environ. Sci. Technol.* **43** (2009) 1250 (https://doi.org/10.1021/es802764g)
15. L. Tan, Q. Liu, X. Jing, J. Liu, D. Song, S. Hu, L. Liu, J. Wang, *Chem. Eng. J.* **273** (2015) 307 (https://doi.org/10.1039/C7RA07260K)
16. C. Hong Chen, Y. H. Liang, W. D. Zhang, *J. Alloy Compd*. **501** (2010) 168 (https://doi.org/10.1039/C1RA00260K)
17. M. Hosseini, M.Aghazadeh, M. R. Ganjali, *New J. Chem.* **41** (2017) 12678 (http://dx.doi.org/10.1039/C7NJ02082A)
18. M. Arvand, Sh. Hemmati, *Sensors Actuators, B* **238** (2017) 346 (https://doi.org/10.1016/j.snb.2016.07.066)
19. D. S. Mathew, R. S. Juang, *Chem. Eng. J.* **129** (2007) 51 (http://dx.doi.org/10.1016/j.cej.2006.11.001)
20. B. Unal, M. Senel, A. Baykal, H. Sözeri, *Curr. Appl. Phys.* **13** (2013) 1404 (https://doi.org/10.1016/j.cap.2013.04.020)
21. A. A. Ensafi, B. Saeid, B. Rezaei, A. R. Allafchian, *Ionics* **21** (2015) 1435 (https://doi.org/10.1007/s11581-014-1291-0)
22. L. AsadiKafshgari, M. Ghorbani, A. Azizi, S. Agarwald, V. Kumar Gupta, *J. Mol. Liquids* **233** (2017) 370 (https://doi.org/10.1016/j.molliq.2017.03.047)
23. M. B. Gholivand, A. Akbari, M. Faizi, F. Jafari, *J. Electroanal. Chem.* **796** (2017) 17 (https://doi.org/10.1016/j.jelechem.2017.05.004)

24. A. Hirsch, *Angew. Chem. Int. Ed.* **41** (2002)1853 (https://doi.org/10.1002/1521-3773(20020603)41:11<1853::AID-ANIE1853>3.0.CO;2-N)

25. H. Fayazfar, A. Afshar, A. Dolati, *Mater. Sci. Appl.* **4** (2013) 667 (http://dx.doi.org/10.4236/msa.2013.411083)

26. M. Zahraei, A. Monshi, D. Shahbazi-Gahrouei, M. Amirnasr, B. Behdadfar, M. Rostami, *J. Nanostruct.* **5** (2015) 77 (https://doi.org/10.7508/jns.2015.02.001)

27. B. H. Hameed, M. I. El-Khaiary, *J. Hazard. Mater.* **159** (2008) 574 (https://doi.org/10.1016/j.jhazmat.2008.02.054)

28. S. EngLagergren, *Handlingar* **24** (1898) 1.

29. Y. S. Ho, G. McKay, *Chem. Eng. J.* **70** (1998) 115 (https://doi.org/10.1016/S0923-0467(98)00076-1)

30. Y. Zhou, Y. Min, H. Qiao, Q. Huang, E. Wang, T. Ma, *Int. J. Biolog. Macromol.* **74** (2014) 271 (https://doi.org/10.1016/j.ijbiomac.2014.12.020)

31. L. Ai, H. Huang, Z. Chen, X. Wei, J. Jiang, *Chem. Eng. J.* **156** (2010) 243 (https://doi.org/10.1016/j.cej.2009.08.028)

32. M. Ghaedi, F. Nasiri Azad, K. Dashtian, S. Hajati, A. Goudarzi, M. Soylak, *Spectrochim. Acta, A* **167** (2016) 157 (https://doi.org/10.1016/j.saa.2016.05.025)

33. X. Zhang, H. Yu, H. Yang, Y. Wan, H. Hu, Z. Zhai, J. Qin, J *Colloid Interf. Sci.* **437** (2015) 277 (https://doi.org/10.1016/j.jcis.2014.09.048)

34. E. Sharifpour, H. Z. Khafri, M. Ghaedi, A. Asfaram, R. Jannesar, *Ultrason. Sonochem.* **40** (2018) 373(https://doi.org/10.1016/j.ultsonch.2017.07.030)

35. F. Bouaziza, M. Koubaab, F. Kallela, R. EllouzGhorbela, S. EllouzChaabouni, *Int. J. Biolog. Macromol.* **105** (2017) 56 (https://doi.org/10.1016/j.ijbiomac.2017.06.106)

36. I. Langmuir, *J. Am. Chem. Soc.* **38** (1916) 2221(https://doi.org/10.1021/ja02268a002)

37. H. M. F. Freundlich, *J. Phys. Chem.* **57** (1906) 385.

38. F. Haghseresht, G. Lu, *Energy Fuels* **12** (1998) 1100 (https://doi.org/10.1021/ef9801165).